

## Self-emerging and turbulent chimeras in oscillator chains

Grigory Bordyugov,<sup>\*</sup> Arkady Pikovsky, and Michael Rosenblum

*Institut für Physik und Astronomie, Universität Potsdam, Karl-Liebknecht-Straße 24/25, 14476 Potsdam, Germany*

(Received 2 March 2010; revised manuscript received 10 September 2010; published 30 September 2010)

We report on a self-emerging chimera state in a homogeneous chain of nonlocally and nonlinearly coupled oscillators. This chimera, i.e., a state with coexisting regions of complete and partial synchrony, emerges via a supercritical bifurcation from a homogeneous state. We develop a theory of chimera based on the Ott-Antonsen equations for the local complex order parameter. Applying a numerical linear stability analysis, we also describe the instability of the chimera and transition to phase turbulence with persistent patches of synchrony.

DOI: [10.1103/PhysRevE.82.035205](https://doi.org/10.1103/PhysRevE.82.035205)

PACS number(s): 05.45.Xt, 05.65.+b

Populations of coupled oscillators is a paradigmatic model of nonlinear science, with numerous applications from purely physical ones such as Josephson junction arrays and coupled lasers to biologically and even socially important [1]. One of the most spectacular recent findings are the so-called *chimera* states (CSs) which are observed in otherwise completely synchronizable oscillatory media if the system starts from certain initial states. CSs are characterized by the coexistence of complete and partial synchrony in homogeneous spatially extended systems. CSs were initially discovered and explained theoretically in [2], and then received more analytical treatment in [3]. Following those pioneering works on CSs, a large body of observations and analysis of similar regimes has been recently published, see [4].

In this paper, we add another species to the zoo of chimeras. The crucial difference is that our CS does not coexist with a stable completely synchronous state. It emerges from a general initial state and is thus denoted as self-emerging. CS is stable close to the bifurcation, but with a further variation of the parameter it becomes turbulent, so that synchronous and partially synchronous patches intermingle irregularly. The key elements of our model are Stuart-Landau oscillators, coupled through a decaying kernel as in the original chimera setup, but with a difference that the coupling is *nonlinear* in the sense of [5]. We numerically demonstrate the existence of CS and explain it in the phase dynamics framework with the help of reduced equations for the local order parameter. Our main theoretical tools are the equations for the complex order parameter in the so-called Ott-Antonsen (OA) equations [6]. They exploit a parametrization of the probability density for ensembles of sinusoidally coupled phase oscillators and result in a closed equation for the order parameter. The OA theory is closely related to the Watanabe-Strogatz theory [7] which is exact but does not yield closed equations in terms of the order parameter. A connection between these two theories has been established in [8].

As a basic model we consider a one-dimensional, periodic in space chain of the length  $L=2\ell$  of nonlocally coupled identical Stuart-Landau oscillators

$$\partial_t A = (1 + i\tilde{\omega})A - |A|^2 A + \varepsilon Z, \quad (1)$$

where  $A=A(x,t)$  is the complex amplitude,  $\tilde{\omega}$  is the natural frequency of the oscillators,  $Z=Z(x,t)$  is the coupling force acting on the oscillator at  $x$ , and  $\varepsilon$  is a small coupling constant. The coupling is organized via a convolution of  $A(x,t)$  with the weight function  $G(x)=ce^{-|x|}$ ,

$$B(x,t) = \int_{-\ell}^{\ell} dx' G(x-x') A(x',t), \quad (2)$$

where the constant  $c$  ensures that  $\int_{-\ell}^{\ell} G(x)dx=1$ . The forcing is then defined as

$$Z = e^{i\beta(|B|)} B. \quad (3)$$

The phase shift  $\beta(|B|)=\beta_0+\beta_1|B|^2$ , chosen in spirit of [5], accounts for possible nonlinearity effects in the coupling, i.e., the dependence of the forcing  $Z$  in Eq. (1) on the higher-order powers of  $B$ . The weight function  $G(x)$  is kept fixed, so that by variation of  $L$  we change the ratio between the coupling width and the system size.

We integrated Eqs. (1)–(3) using  $2^{17}$  sites in  $x$  with  $\varepsilon=0.01$ ,  $\tilde{\omega}=0$ ,  $\beta_0=0.4\pi$  and  $\beta_1=(\pi/2-\beta_0)/0.36$  (this choice of  $\beta_1$  will be apparent later on) using the Runge-Kutta fourth order scheme. Initial conditions were chosen randomly close to the completely desynchronized state. To measure the synchronization between adjacent oscillators on a mesoscopic scale, we calculated the coarse-grained  $\bar{A}(x,t)$  by averaging  $A(x,t)$  over  $2^{10}$  closest neighbors. For small  $L$ , we observed a spatially homogeneous, uniformly rotating self-organized quasiperiodic (SOQ) state with  $|\bar{A}|=|B|\approx 0.6$ , like in globally coupled ensembles [5]. This state becomes unstable if the system size  $L$  exceeds the critical value  $L_c\approx 5.1$ . For  $L>L_c$ , a spatially modulated profile of  $|B|$  emerged, see Fig. 1(a). The profile of  $|\bar{A}|$  was stationary up to finite-size fluctuations. Close to the transition, synchronization was only partial, with  $|\bar{A}|<1$  for all  $x$ . For  $L\geq 5.35$ , the profile of  $|\bar{A}|$  reached unity [see Fig. 1(b)]: all oscillators in that region were completely synchronized. In the regions with  $|\bar{A}|<1$  the local synchronization was only partial. Such state is a stationary chimera [2,3]. With further increase of  $L$ , this regime becomes unstable and evolves into a turbulent state where synchronized patches with  $|\bar{A}|\approx 1$  appeared at random places and disappeared after some time, see Figs. 1(c)–1(e). We call

<sup>\*</sup>grigory.bordyugov@uni-potsdam.de

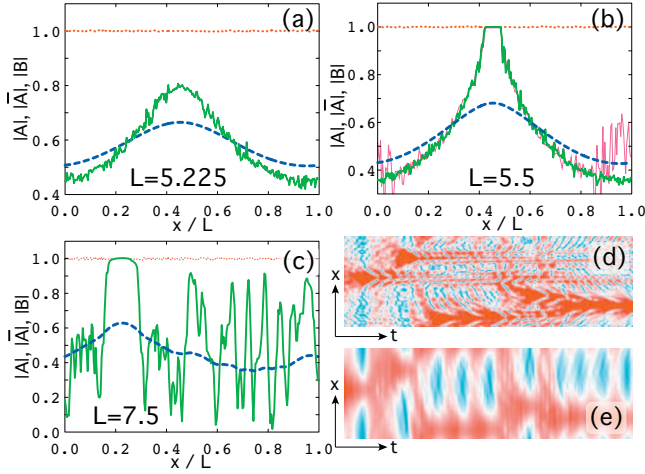


FIG. 1. (Color) Results of simulation of Eq. (1). (a) and (b) show stationary patterns, (c)–(e) show a turbulent one. In (a)–(c) we show profiles of  $|A|$  (dotted red line),  $|\bar{A}|$  (solid green line), and  $|B|$  (long-dashed blue line). The system size  $L$  is specified in each frame. In (b), thin pink solid line (largely occluded by the green one) shows a snapshot from simulation with specially prepared initial state, see text. In panels (d) and (e), showing space-time plots of  $|\bar{A}|$  and  $|B|$ , respectively, red color (darker in b/w print) encodes values close to 1, blueish color (brighter in b/w print) encodes values close to 0. In (d) and (e), the time span of simulations is 5000 dimensionless time units and  $L=7.5$ .

this state a *turbulent chimera*. Below, we present a theoretical description of stationary CSs in terms of a reduced phase model.

For small coupling  $\varepsilon$ , we can assume that the amplitude of each Stuart-Landau oscillator remains unperturbed and the system can be described solely by its phase  $\theta(x, t)$ . In the thermodynamic limit, the population is described by a probability density distribution  $\rho = \rho(x, \theta, t)$ . This density obeys the continuity equation  $\partial_t \rho + \partial_\theta(\rho v) = 0$  with the velocity field  $v(x, \theta, t) = \dot{\theta} = \omega + \text{Im}(Z(x, t)e^{-i\theta})$ , where we rescaled the coupling parameter  $\varepsilon \rightarrow 1$  by rescaling time and frequency by  $t \rightarrow \varepsilon t$ ,  $\omega = \tilde{\omega}/\varepsilon$ . Next, we define the complex order parameter by

$$z(x, t) = r e^{i\varphi} = \int_0^{2\pi} d\theta e^{i\theta} \rho(x, \theta, t),$$

so that  $B(x, t)$  is expressed as

$$B(x, t) = b(x, t) e^{i\psi(x, t)} = \int_{-\ell}^{\ell} dx' G(|x - x'|) z(x', t). \quad (4)$$

Now we apply the theories developed in [6–8] and use the OA equation for the complex order parameter  $z(x, t)$

$$\partial_t z = i\omega z + \frac{1}{2}(Z - z^2 Z^*). \quad (5)$$

(We justify the applicability of the OA theory towards the end of the paper.) Equation (5) together with Eqs. (3) and (4) constitute a closed system which we analyze to study pattern formation in the domains of various length  $L$ . This system

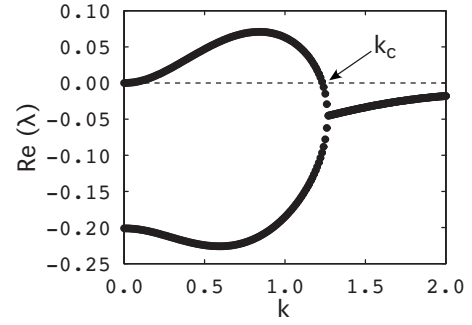


FIG. 2. The real part of the stability eigenvalues  $\lambda$  of  $z_{\text{soq}}$  in dependence on  $k$  (the wave number of perturbation).  $k_c \approx 2\pi/5.10$  denotes the critical wave number.

differs from Eqs. (13) and (14) of Laing in Physica D [4] by the nonlinear phase shift  $\beta$ . With a proper choice of  $\beta_0$  and  $\beta_1$ , Eq. (5) supports three types of homogeneous steady states: (i) The completely desynchronized one  $z_0 = 0$ , (ii) the fully synchronized one  $z_1 = e^{i\Omega_1 t}$  with  $\Omega_1 = \omega + \sin(\beta_0 + \beta_1)$ , and (iii) the intermediate regime of SOQ [5]  $z_{\text{soq}} = r_{\text{soq}} e^{i\Omega_{\text{soq}} t}$  with  $r_{\text{soq}} = \sqrt{\frac{\pi/2 - \beta_0}{\beta_1}}$  and  $\Omega_{\text{soq}} = \omega + \frac{1}{2}(1 + r_{\text{soq}}^2)$ . Due to the normalization of the kernel  $G$ ,  $z_0$ ,  $z_1$ , and  $z_{\text{soq}}$  persist for all  $\ell$ . Knowing from [5] that both  $z_0$  and  $z_1$  are unstable, we focus on  $z_{\text{soq}}$ . A linear stability analysis of  $z_{\text{soq}}$  with the perturbation  $\propto y e^{\lambda t + i k x}$  results in the eigenvalue problem

$$\lambda \begin{pmatrix} y e^{i k x} \\ y^* e^{-i k x} \end{pmatrix} = \frac{1}{2} \begin{pmatrix} \mathcal{L}_{11} & \mathcal{L}_{12} \\ \mathcal{L}_{12}^* & \mathcal{L}_{11}^* \end{pmatrix} \begin{pmatrix} y e^{i k x} \\ y^* e^{-i k x} \end{pmatrix},$$

where  $\mathcal{L}_{11} = \{i(r_{\text{soq}}^2 - 1) + \alpha(k, \ell)[i - \beta_1 r_{\text{soq}}^2(1 - r_{\text{soq}}^2)]\}$  and  $\mathcal{L}_{12} = \alpha(k, \ell)[i r_{\text{soq}}^2 - \beta_1 r_{\text{soq}}^2(1 - r_{\text{soq}}^2)]$  with the  $\ell$ -dependent wave number factor

$$\alpha(k, \ell) = \frac{1 + e^{-\ell}[k \sin(k\ell) - \cos(k\ell)]}{(1 - e^{-\ell})(1 + k^2)}, \quad (6)$$

which converges to  $(1 + k^2)^{-1}$  as  $\ell \rightarrow \infty$ . The eigenvalues  $\lambda_{1,2}$  of matrix  $\mathcal{L}$  depend on both  $k$  and  $\ell$ . On the infinite domain, we find that  $\text{Re } \lambda_1(k, \infty) > 0$  and  $\text{Im } \lambda_{1,2}(k, \infty) = 0$  for  $0 < k < k_c$  with the critical wave number  $k_c = \sqrt{\frac{\pi - 2\beta_0}{\beta_1 + \beta_0 - \pi/2}}$ . With a finite  $\ell$ , the critical wave number differs from  $k_c$  since  $\ell$  enters  $\alpha(k, \ell)$ . The critical system length  $L_c = 2\ell_c$  at which the instability occurs, is determined by the condition  $\text{Re } \lambda(\pi/\ell_c, \ell_c) = 0$ . To exemplify the instability, we chose  $\beta_0 = 0.4\pi$  and  $\beta_1$  such that  $\beta_0 + \beta_1 \times 0.6^2 = \pi/2$ , so that  $r_{\text{soq}} = 0.6$  (cf. numerics of Fig. 1). Solving the eigenvalue problem, we obtained the critical length  $L_c \approx 5.09$  (see Fig. 2) in a nice correspondence with the results of the direct numerical simulations.

The instability described above results in uniformly rotating spatially inhomogeneous regimes, thus we look for solution  $z_{\text{ch}}(x, t) = r(x) e^{i[\Omega t + \varphi(x)]}$  with unknown  $\Omega$ ,  $r(x)$  and  $\varphi(x)$ . For the forcing we assume  $B(x, t) = b(x) e^{i[\Omega t + \psi(x)]}$ . When substituting this in Eq. (5), we have to distinguish between two cases: (i) for regions with  $r < 1$  the stationarity/stability conditions yield

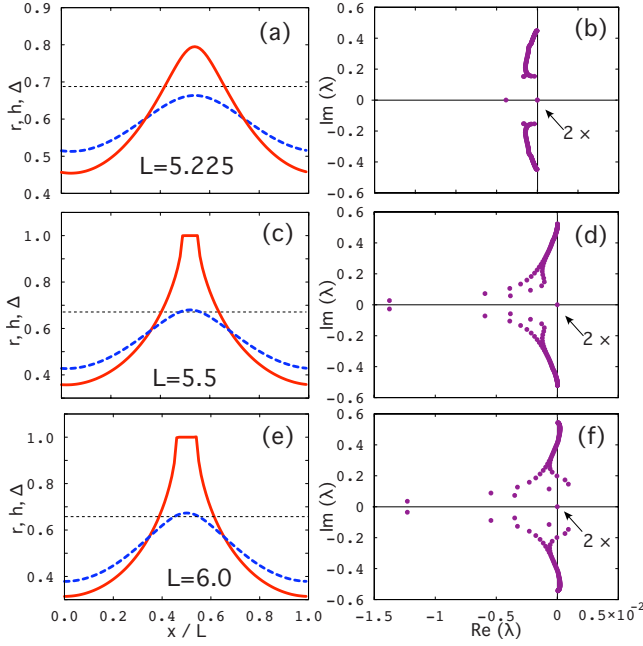


FIG. 3. (Color online) Stationary profiles of  $r$  for different system sizes  $L$ . On the left,  $r=|z|$  (solid red line) and  $b$  (dashed blue line) in comparison to  $\Delta$  (horizontal short-dashed line) are depicted, the corresponding stability eigenvalues of the Jacobian matrix are on the right.

$$r(x) = \Gamma(x) - \sqrt{\Gamma^2(x) - 1},$$

$$\varphi(x) = \psi(x) + \beta[b(x)] - \pi/2, \quad (7)$$

with the detuning  $\Delta = \Omega - \omega$ ; (ii) for regions with  $r=1$  we have

$$\varphi(x) = \psi(x) + \beta[b(x)] + \arcsin \Gamma(x), \quad (8)$$

where in both Eqs. (7) and (8)  $\Gamma(x) = \Delta/b(x)$ . Equations (7) or (8) plus Eq. (4) constitute a closed system, which we could not solve analytically. Instead, we found the stationary CSs in the frame rotating with frequency  $\Omega$ , employing the Newton's method for Eq. (5) discretized in  $x$ . In the Newton's calculations, an additional phase pinning condition was imposed in order to pick up a unique solution from the family of phase rotations. The number of unknowns and equations was then balanced by taking  $\Omega$  as an additional unknown. After the solution  $z_{\text{ch}}(x)$  had been found with a desired accuracy, we looked at its linear stability by computing the eigenvalues  $\lambda$  of the Jacobian matrix evaluated at  $z_{\text{ch}}(x)$ . Eigenvalues with positive real parts signalize an instability of  $z_{\text{ch}}(x)$ . For smaller  $L$  close to  $L_c$ , the profile of  $z_{\text{ch}}(x)$  shows a moderate sinelike modulation, see Fig. 3(a). For larger  $L$ , the profile of  $z_{\text{ch}}(x)$  touches unity: a patch of complete synchronization emerges; this is a genuine CS. This occurs in the region with  $b > \Delta$ , see Fig. 3(c). For our choice of  $\beta_0$  and  $\beta_1$ , the regimes with  $r < 1$  for all  $x$  are linearly stable [see Fig. 3(a) and 3(b)], whereas the CS with a synchronized patch with  $r=1$  destabilizes as  $L$  increases, cf. Figs. 3(c)–3(f). We believe that this instability is inherited

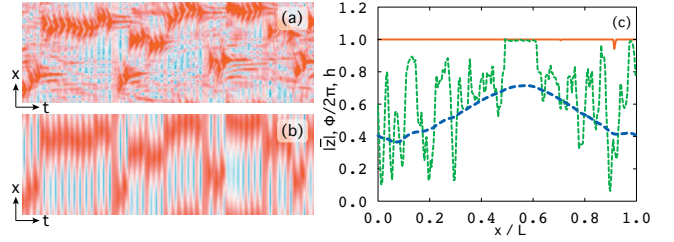


FIG. 4. (Color) Space-time plots of the coarse-grained order parameter  $|\bar{z}|$  (a) and of  $b$  (b) obtained by numerical integration of Eq. (5) with  $L=7.5$ . Red color (darker in b/w print) represents larger values close to one, bluish (brighter in b/w print) represents smaller values close to zero. We show simulation results from 1500 to 3000 dimensionless time units. The discretization in space  $x$  was done on 1024 sites. (c) Final snapshot of integration from (a) and (b): Solid red line shows non-coarse-grained  $r=|z|$ , green short-dashed line shows the magnitude of the coarse-grained  $\bar{z}$ , and long-dashed blue line represents profile of  $b$ .

from the instability of  $z_1$ , due to the presence a plateau of complete synchronization with  $|z|=1$ .

Numerical simulations of Eq. (5) show that beyond the instability of the stationary CS, a turbulent state occurs, where a synchronous patch is persistent but appears at different places. We call this state a turbulent chimera. Figures 4(a) and 4(b) show a result of numerical integration of Eq. (5) for  $L=7.5$ . Since the order parameter  $z$  must be a coarse-grained quantity, in numerical simulations we average the  $z$  field over a small spatial interval (in our simulation over 16 neighboring sites) to get  $\bar{z}$ . In Fig. 4(a), the red patches with coarse-grained  $|\bar{z}|$  close to one show a larger degree of local coherence of oscillators in comparison to the blueish rest. These coherent regions persist, allowing us to characterize the irregular state as a chimera turbulence. The forcing magnitude  $b$  [cf. Fig. 4(b)] does not show any saturation, irregularly oscillating between smaller (blue color) and larger (red color) values. A typical final snapshot of the system is shown in Fig. 4(c). There is a fully synchronous patch near  $x/L \approx 0.5$  where  $|\bar{z}| \approx 1$ .

Now we comment on the applicability of the OA Eq. (5), since for identical oscillators under a common forcing the ensemble dynamics can fall beyond the OA theory [8]. For nonidentical oscillators,  $\rho(x, \theta, t)$  asymptotically fulfills the conditions for the OA theory (one says that a solution is attracted to the invariant OA manifold) [6]. Here, even though the oscillators are identical, the force that acts on them is inhomogeneous in space [see profiles of  $|B|$  in Fig. 1(b)], which plays the same mixing role as the nonidentity of oscillators in [6] and the phase distribution tends to the OA manifold as well. Indeed, consider the unsynchronized dynamics of the phase  $\theta(x, t)$  under forcing  $Z=b(x)e^{i(\Omega t + \tilde{\psi}(x))}$  which is uniformly rotating in time and inhomogeneous in  $x$ :

$$\partial_t \theta(x) = \omega + b(x) \sin[\Omega t - \theta(x) + \tilde{\psi}(x)].$$

We transform to a uniformly rotating phase  $\phi[\theta(x)]$  by

$$\phi(\theta) = 2 \arctan \frac{(\omega - \Omega) \tan[(\theta - \tilde{\psi})/2] - b}{[(\omega - \Omega)^2 - b^2]^{1/2}},$$

with  $\partial_t \phi = [(\omega - \Omega)^2 - b^2]^{1/2}$ , which immediately results in the solution  $\phi(x, t) = \phi(x, 0) + t [(\omega - \Omega)^2 - b^2]^{1/2}$ . We characterize the distribution of  $\phi$  with the help of its  $m$ th order parameter given by  $\langle e^{im\phi(x,t)} \rangle = \langle e^{im\phi(x,0)} \rangle \langle e^{imt((\omega - \Omega)^2 - b^2(x))^{1/2}} \rangle$  (the brackets  $\langle \cdot \rangle$  denote averaging over small  $x$  neighborhood as described above). The second average in the product asymptotically vanishes for  $t \rightarrow \infty, m \neq 0$  (here, we explicitly used the nonuniformity of the forcing  $Z$ ) and hence for large  $t$  the distribution of  $\phi(x, t)$  is uniform. This in turn results in  $\rho(\theta, x, t)$  being on the OA manifold, see [7,8]. Our derivation is valid only for stationary forcing, in contrast to the more general analysis of [6]. Additionally, we ran a simulation with initial condition that strongly violated the OA theory. This run also resulted in a stationary CS. The profile of  $|B|$  was indistinguishable from the previous simulation with nearly uniform initial distribution of phases. The profile of  $|\bar{A}|$  [thin solid pink line in Fig. 1(b)] is close to the previous one up to the finite-size fluctuations in the region of small  $|B|$  values. The differences in  $|\bar{A}|$  are mostly pronounced in the domain with nearly uniform forcing  $|B|$ , what agrees with the aforementioned reasoning. We also followed the deviation from the OA manifold looking at the quantity  $|\langle e^{i\theta} \rangle^2 - \langle e^{i2\theta} \rangle|$ , which vanishes on the OA manifold. We found that even for

initial conditions off the OA manifold, asymptotically it always decreased in time.

Our results can be extended to nonidentical oscillators with a Lorentzian distribution of frequencies. In this case the OA theory yields Eq. (5) with an additional damping term (so that the eigenvalue spectra of CS move from the imaginary axis into the left complex half-plane), which results in very similar states with the difference that synchronization is never complete.

Summarizing, we have demonstrated the existence of chimeralike solutions in chains of nonlocally and nonlinearly coupled oscillators. In our system, chimera appears as a result of a long-wavelength instability via a supercritical bifurcation. Unlike the previously reported CSs (except for CSs in ensembles of Hodgkin-Huxley neurons in Sakaguchi [4]), we do not need to prepare initial conditions to avoid complete synchrony, because it is unstable. CSs can be asymptotically described within the OA theory even if the initial condition is not on the OA manifold. As the stationary chimera becomes unstable, it evolves into a turbulent one. In this regime the complex order parameter changes irregularly in space and time, but nevertheless the patches of synchronization appear persistently. This characterizes the chimera as an important pattern in the dynamics of nonlinearly coupled oscillators.

We acknowledge financial support from DFG via SFB 555 and useful discussions with Yu. Maistrenko, E. Martens, O. Omel'chenko, M. Wolfrum, and B. Fiedler.

- 
- [1] Y. Kuramoto, *Chemical Oscillations, Waves and Turbulence* (Dover, New York, 2003); A. Pikovsky, M. Rosenblum, and J. Kurths, *Synchronization: A Universal Concept in Nonlinear Science* (Cambridge University Press, Cambridge, 2001); S. Strogatz, *Sync: The Emerging Science of Spontaneous Order* (Hyperion, New York, 2003); J. A. Acebrón *et al.*, *Rev. Mod. Phys.* **77**, 137 (2005).
- [2] Y. Kuramoto and D. Battogtokh, *Nonlinear Phenom. Complex Syst.* (Dordrecht, Neth.) **5**, 380 (2002).
- [3] D. M. Abrams and S. H. Strogatz, *Phys. Rev. Lett.* **93**, 174102 (2004); *Int. J. Bifurcation Chaos Appl. Sci. Eng.* **16**, 21 (2006).
- [4] S.-I. Shima and Y. Kuramoto, *Phys. Rev. E* **69**, 036213 (2004); Y. Kawamura, *ibid.* **75**, 056204 (2007); H. Sakaguchi, *ibid.* **73**, 031907 (2006); O. E. Omel'chenko, Y. L. Maistrenko, and P. A. Tass, *Phys. Rev. Lett.* **100**, 044105 (2008); G. C. Sethia, A. Sen, and F. M. Atay, *ibid.* **100**, 144102 (2008); D. M. Abrams, R. Mirollo, S. H. Strogatz, and D. A. Wiley, *ibid.* **101**, 084103 (2008); C. R. Laing, *Chaos* **19**, 013113 (2009); *Physica D* **238**, 1569 (2009).
- [5] M. Rosenblum and A. Pikovsky, *Phys. Rev. Lett.* **98**, 064101 (2007); *Physica D* **238**, 27 (2009).
- [6] E. Ott and T. M. Antonsen, *Chaos* **18**, 037113 (2008); **19**, 023117 (2009).
- [7] S. Watanabe and S. H. Strogatz, *Phys. Rev. Lett.* **70**, 2391 (1993); *Physica D* **74**, 197 (1994).
- [8] A. Pikovsky and M. Rosenblum, *Phys. Rev. Lett.* **101**, 264103 (2008); e-print arXiv:1001.1299.